

NUMERICAL MODELING OF WAVE-CURRENT INTERACTION IN TIDAL AREAS USING AN UNSTRUCTURED FINITE VOLUME TECHNIQUE

Ole R. Sørensen¹, Henrik Kofoed-Hansen¹ and Oliver P. Jones²

The present paper describes applications of an integrated numerical modeling system for the study of hydrodynamic conditions in areas with large tidal and surge variations, strong current and very complex bathymetries. The modeling system includes a dynamic coupling between a 2D flow model and a spectral wave model and is based on an unstructured finite volume technique. Two applications are presented: the Bristol Channel, United Kingdom, and Grådyb tidal inlet, Denmark, characterized as macro- and micro-tidal estuaries, respectively. The work demonstrates the advantages of using an unstructured grid approach and that the inclusion of wave-current interaction is mandatory for obtaining accurate results in tidal areas.

INTRODUCTION

Successful prediction of hydrodynamic conditions and morphological changes in tidal areas requires detailed knowledge of water and sediment movement. Many tidal areas are controlled by complex hydrodynamic conditions in which tide, swell, wind waves and wind stress have significant forcing effects on the system. Very often the flow pattern consists of the combined interaction of tidal currents and a wave induced current field. The complexity is further enhanced by the influence of the flow field on wave propagation.

Recently, spectral wave models have been extended to application in coastal areas. Improvements in the physical description of processes and the use of new solution techniques (e.g. flexible mesh) have made it possible to apply coupled flow and spectral wave models to a wide range of complex coastal conditions.

In this paper we shall focus on simulating the interaction between waves and currents using a dynamic coupling between a fully spectral wave model and a 2D flow model. Both models are based on an unstructured cell-centered finite volume method and use an unstructured mesh in geographical space.

Compared to flow modeling, the computational cost of spectral wave modeling is relatively high. Setup of a spectral wave model, therefore, is often a compromise between accuracy and performance: A fine resolution model may improve the results, but may be computationally prohibitive. One way to reduce the computational cost is to solve the wave formulations using a quasi-stationary formulation as an alternative to a full instationary formulation. The quasi-stationary approach performs a series of time-independent solutions throughout

¹ DHI Water & Environment, Agern Allé 5, Hørsholm, DK 2970, Denmark

² University College London, Gower Street, London, WC1E6BT, UK

a tidal cycle, which incorporate the effects of dynamic currents and water levels. The quasi-stationary solution is based on the ‘stationary assumption’ which assumes an aphysical instantaneous travel time of wave energy across the model domain and that waves respond instantaneously to changes in the wind field. Such an approach is usually satisfactory for coastal studies, however in larger domains, the stationary assumption becomes invalid and an instationary (time-dependent) solution must be used.

In this study, we test the validity of using a new, computationally efficient, quasi-stationary approach for combined wave-current modeling in two complex case studies. These include the Bristol Channel, a very large, ebb-dominated, macro-tidal estuary in the Western U.K., and the micro-tidal Grådyb inlet located in the Danish part of the Wadden Sea.

MODELING SYSTEM

The spectral wave model MIKE 21 SW, is part of the MIKE 21/3 Coupled Model FM. It is a truly dynamic modeling system for application within coastal and estuarine environments. The flow and spectral wave models are the basic computational components of the modeling system. The flow model permits both 2D and 3D flows to be simulated and the combined wave-current system simulates the mutual interaction between waves and currents using a dynamic coupling. The same system can also be coupled to a sediment transport model to provide feedback between bed level changes and the hydrodynamics. The numerical approach applied in both the wave and flow models is based on a cell-centered finite volume technique on an unstructured grid.

Flow model

The flow model solves the 2D shallow water equations. The effect of waves on the flow field is taken into account by the radiation stress gradients. The radiation stresses are obtained from the wave model using a spectral formulation (Battjes, 1972).

The shallow water equations are solved using a second-order scheme. An approximate Riemann solver (Roe’s scheme, see Roe, 1981) is used to calculate the convective fluxes. Second-order spatial accuracy is achieved by employing a linear gradient-reconstruction technique. The average gradients are estimated using the approach by Jawahar and Kamath, 2000. To avoid numerical oscillations a second-order TVD slope limiter (Van Leer limiter, see Hirsch, 1990) is used. A second-order Runge-Kutta method is used for the time integration.

Spectral wave model

The spectral wave model includes two different formulations: a fully spectral formulation and a directionally decoupled parameterized formulation of the wave action balance equation. The fully spectral formulation is used in the present work. In the fully spectral formulation the source functions are based on the WAM Cycle 4 formulations (see Komen et al. 1994). The source term for

depth-limited wave breaking is based on the formulation by Battjes et al., 1978. A short description of the source terms can be found in Sørensen et al., 2004. The effect of the time-varying depth and currents is taken into account by the formulation of propagation speeds in the geographical and spectral spaces. The spectral wave model is parallelized using OpenMP technique.

The conservation equation for wave action is solved using a first-order scheme. A first-order upwinding scheme is employed to calculate the convective fluxes both in geographical and spectral space. For the instationary equations the time integration is based on a fractional step approach, where the propagation step is solved using an explicit Euler method. The use of an explicit method can introduce a severe restriction on the time step for a given spatial discretization due to the CFL stability condition. In order to relax the restriction on the time step, a multi-sequence explicit integration scheme is applied. For a more detailed description of the numerical scheme, see Sørensen et al., 2004.

The present paper compares the performance of a new, and more efficient, steady-state or ‘quasi-stationary’ approach, with that of a full instationary solution. Comparisons have also been made between the performance of a full spectral formulation and that of a parametrically-decoupled approach in which the frequency domain is described in terms of a mean-wave frequency.

Solving the set of non-linear equations

$$\bar{F}(\bar{x}) = \bar{0} \quad (1)$$

where $\bar{x} = \{x_1, x_2, \dots, x_N\}$ and $\bar{F} = \{F_1(\bar{x}), F_2(\bar{x}), \dots, F_N(\bar{x})\}$, a modified Newton-Raphson iteration can be expressed as

For $k = 0, 1, 2 \dots$ until convergence, do:

$$\bar{A} \Delta \bar{x}^{k+1} = -\bar{F}(\bar{x}^k) \quad (2)$$

$$\bar{x}^{k+1} = \bar{x}^k + \alpha \Delta \bar{x}^{k+1} \quad (3)$$

Here \bar{A} is an approximation to the Jacobian ($J_{ij} = \partial F_i / \partial x_j$) of the operator \bar{F} with respect to the dependent variables \bar{x} and α is a relaxation factor. The matrix \bar{A} is obtained from the convective terms in geographical space and the diagonal part of the functional derivative of the source terms due to bottom friction, wave breaking and non-linear transfer (fully spectral formulation). The relaxation factor must be in the range from 0 to 1. A value of 0.1 has been shown to give a stable and fast convergence in most cases.

The iteration procedure is stopped when the root-mean-square (RMS) norm of a residual vector and the max-norm of the vector containing the increment of

the significant wave height between two iteration steps are smaller than two user-specified tolerances

$$\left\| \bar{F}(\bar{x}^{k+1}) \right\|_{RMS} < TOL_1 \quad \text{and} \quad \left\| \bar{H}_{m0}^{k+1} - \bar{H}_{m0}^k \right\|_{\max} < TOL_2 \quad (4)$$

In the present work $TOL_1=10^{-5}$ and $TOL_2=0.01$ have been used. The linear system in each iteration step is solved using a marching procedure. This is utilized by a simple upwinding approach which discretizes the convective terms and determines a calculation sequence for each discrete direction. This allows the linear system, Eq. (2), to be solved with a single sweep through the domain for each discrete direction.

Dynamic coupling

The time steps for the flow model and the instationary spectral wave model are dynamic and each determined to satisfy separate CFL stability criterion. The two time steps are synchronized at an overall discrete time step at which information between the two models is exchanged. First, flow computations are performed over the overall time step, keeping the radiation stress gradients constant. Then, time integration for the overall time step is performed for the spectral wave model using a linear interpolation of the water level and current conditions. When the spectral wave model is applied in quasi-stationary mode, a steady-state solution is calculated for each overall time step.

BRISTOL CHANNEL

The Bristol Channel is an ebb-dominated, macro-tidal estuary in the Western U.K., characterized by a series of prominent headlands and large sandy embayment's. The main area of interest is the Swansea Bay (see Figures 1 and 2). Maximum tidal range during peak springs varies from 5m at the mouth of the estuary to 12m in some locations in the upper estuary. In the main area of interest the tidal range is 8 m. The region is subject to long period swell and locally generated wind waves and provides one of the most severe test cases for a coupled wave-current model.

Simulations have been carried out for a number of different wind, wave and tidal conditions. In this paper, however, results will be presented for the period of the 12th to the 24th May 2002. This is a period over which suitable directional wave data are available from a U.K. Met. Office 5 year deployment near the Scarweather Sands, labeled herein as 'Scarweather' (U.K. Met. Office National Centre for Ocean Forecasting, 2005) and flow and wave data at two locations in front of and behind the Scarweather Sands, labeled herein as 'site 1' and 'site 2'. (GARDLINE, Titan Surveys, 2002). The locations of the three stations are shown in Figure 2. The water depth at Scarweather, site 1 and site 2 are 29m, 14m and 26m, respectively.

In order to capture the ebb-dominated macro-tidal characteristics of the region, the model mesh (Figure 1) has been extended from the upper Severn Estuary to an

open, offshore boundary in the Celtic Sea. The node separation varies from approximately 5km in the outer offshore regions to 500m in the main area of interest (Swansea Bay). A close-up of the mesh covering the Swansea Bay area is presented in Figure 2.

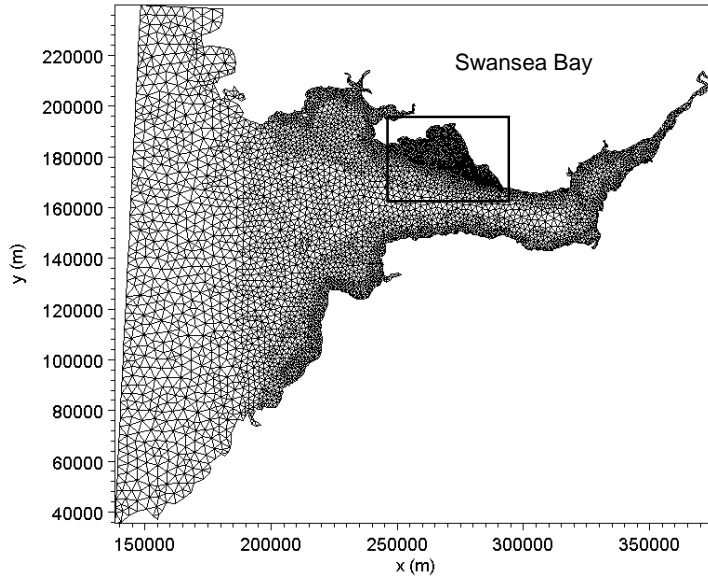


Figure 1. Computational mesh for the Bristol Channel case.

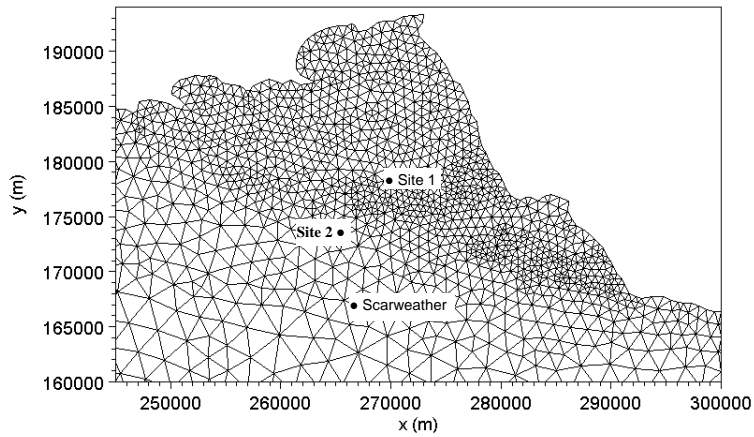


Figure 2. Close-up of the computational mesh for the Bristol Channel case. Swansea bay area.

For the fully spectral experiments, the frequency domain was divided into 30 discrete bins ranging from 0.04 to 0.7 Hz. For the directional domain, 16 discrete directions were selected. For the instationary (time-dependent) experiments, the overall time-step was set to 60 seconds and for the quasi-stationary experiments, stationary computations were performed at intervals of 3600 seconds.

The flow model used tidal elevation data based on global tidal analysis (Andersen, 1995). The spectral wave model used wind sea and swell parameters from the Lundy wave-rider buoy at 51.17N 005.42W (WAVENET, 2002)

Measured wind speeds and directions from the Scarweather wave-rider buoy were used for the wind forcing. A value of $\gamma = 0.8$ was used in the wave breaking formulation, and a Nikuradse roughness of $k_N = 0.05\text{m}$ applied uniformly across the model domain.

Comparisons between modeled and measured water levels and current speeds around the Bristol Channel show, in general, very good agreement. Figure 3 shows comparisons of model predictions with measured current speeds at sites 1 and 2.

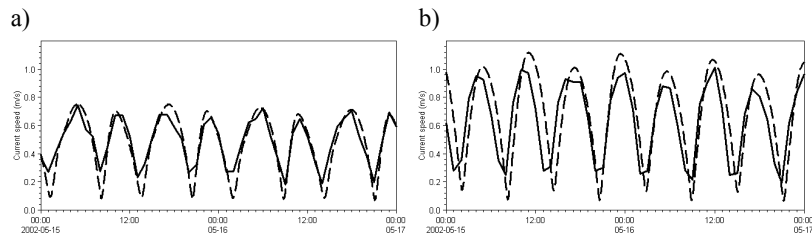


Figure 3. Current speed at site 1 (a) and site 2 (b) for the Bristol Channel case.
— Measurements, - - - Calculations

Time series comparisons of instationary predictions with measured integrated wave parameters at Scarweather are presented in Figure 4. Parameters that have been compared include the significant wave height, H_{m0} , the peak wave period, T_p , the mean wave period, T_{01} , and the peak wave direction, θ_p . The agreement is good although the wave heights are underestimated when the wind is coming from east and south-east. In Figure 5 a time series of the calculated and measured significant wave height, H_{m0} , from site 1 is shown. For comparison, the results of a simulation in which water level and current effects are excluded from the instationary wave calculations are presented (see Figure 5).

The impact of varying water level and current on the model predictions is shown to be significant, particularly on the wave height. However, the coupled flow-wave model underestimates the oscillation amplitude of the wave parameters caused by the tidal variation.

Results of the simulations conducted using the quasi-stationary formulation show excellent agreement with the instationary predictions, particularly at the Scarweather location. Figure 5 shows predictions of significant wave height using the two formulations.

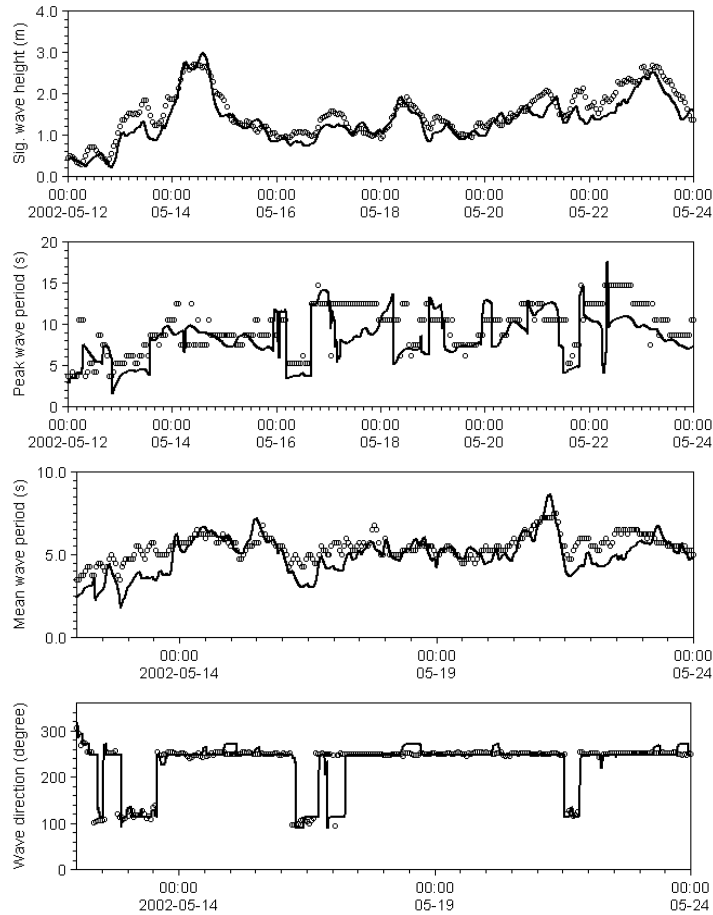


Figure 4. Wave parameters at Scarweather for the Bristol Channel case.
O Measurements, — Calculations (instantaneous formulation).

Generally, the water depths over sandbanks in the Swansea Bay area are very shallow. During low water the depth decreases to less than 2m. The effect of the varying water depth, therefore, is very severe in these areas. Within a tidal period the significant wave height can vary from 0-3m. In the measurement locations, however, the effect of the varying water depth on the waves is limited. Therefore, it is difficult to adequately assess the models performance in these extremely shallow water areas.

Another important factor is the high current speeds that exist over the bank crests. For example, the model predicts maximum current speeds of up to 1.5ms^{-1} .

Under such conditions it is inevitable that wave blocking will occur. We assume that this is the main reason that the model underestimated the effect of tidal variation on the wave heights and periods measured at sites 1 and 2. This is a result of the difficulty in describing the physics of wave conditions close to blocking using a phase-averaged model approach.

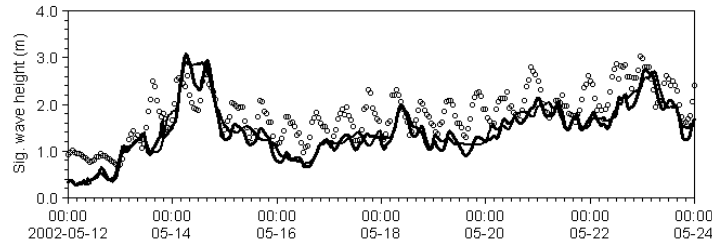


Figure 5. Significant wave height at site 1 for the Bristol Channel case.
O Measurements, **—** Calculations (instantaneous formulation), **- -** Calculations (instantaneous formulation, but excluding level and current effects).

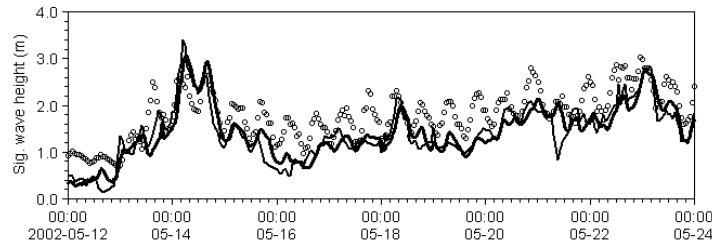


Figure 6. Significant wave height at site 1 for the Bristol Channel case.
O Measurements, **—** Calculations (instantaneous formulation) **- -** Calculations (quasi-stationary formulation).

The computations were carried out on a PC (Pentium D 840 Dual Core, 2x3.2GHz/800/2x1MB). The average time step for the flow calculation was 7.7s, and using the instantaneous formulation, the average time step in the wave calculation was 41.6s. The average number of iterations for the quasi-stationary formulations was 58. For a 12 day simulation, the total CPU time was 51.0 and 25.3 hours for the instantaneous and quasi-stationary solutions respectively. This demonstrates an impressive increase in efficiency that is achievable due to both the stationary assumption and use of the new stationary solver. The elapsed time for the two simulations was 32.4 hours and 18.8 hours, respectively.

GRÅDYB TIDAL INLET

The second case study is the Skallingen barrier spit and the Grådyb tidal inlet (see Figure 7), located in the Danish part of the Wadden Sea. In this area, the

8highest tidal range reaches 1.7m at springs, but the storm surge in the area can be as high as 2-4m. The maximum current in the navigation channel, which leads to the harbor of Esbjerg, is in the range of 1-2m/s. The depth in the channel is 10-12m at mean sea level. The dominant wind directions at the location are west and west-southwest.

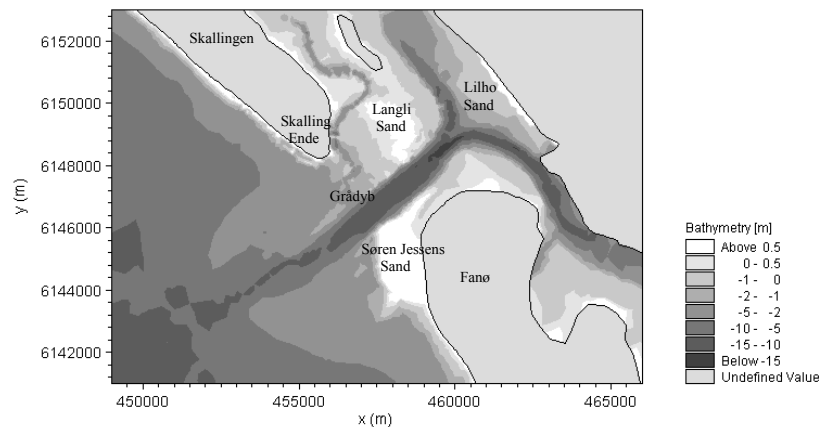


Figure 7. Bathymetry for the Grådyb tidal area.

Simulations have been carried out for a storm event, 2-11 January 1991. During this period the wind direction was in the range 200-270 degree true north and maximum wind speeds of approximately 20 m/s occurred on the 6th and 9th of January. Measurements of wave conditions for this period were carried out at three locations: St. 1 (55° 20' N, 7° 20' E), St. 2. (55° 25,76' N, 8° 12,90' E) and St. 3a (55° 29,05' N, 8° 21,80' E). The water depth at the three stations is 25m, 12m and 10.3m, respectively. The locations of St. 2 and St. 3a are shown in Figure 9.

The mesh contains 20091 elements. The average node separation (edge length) is approximately 1km in the offshore areas and 100m in the shallow areas north and south off the inlet. The mesh is shown in Figure 8 and a close-up of the mesh at the inlet area is shown in Figure 9. For the fully spectral wave formulation, a logarithmic frequency discretization was used including 25 frequencies ranging from 0.05 to 0.85 Hz. The directional space is discretized into 12 directions covering a range from 180 to 360 degrees. For the instationary simulations, the time step was set to 60s and for the quasi-stationary simulations, wave computations were performed at intervals of 3600s.

The boundary conditions for the both the flow and the spectral wave model were obtained from regional simulations covering the North Sea, the Norwegian Sea, the Inner Danish waters, the Baltic Sea and the Gulf of Botnia. A value of $\gamma = 0.8$ was used in the wave breaking formulation, and a Nikuradse roughness of $k_N = 0.05m$, was applied.

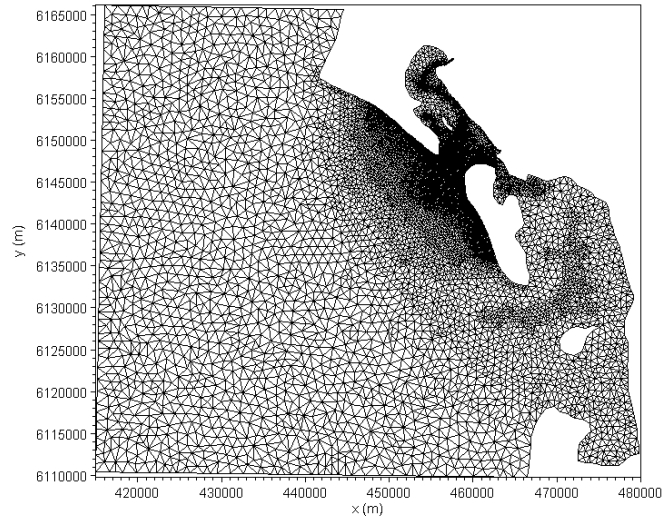


Figure 8. Computational mesh for the Grådyb tidal inlet case.

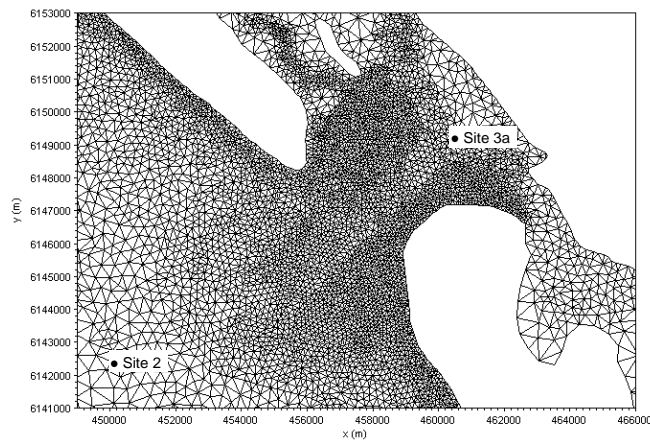


Figure 9. Close-up of the computational mesh for the Grådyb tidal case.

The model shows that shallow water areas including Langli and Søren Jessens Sands to the north of the channel and Skalling Ende to the south of the channel dried at low tide and flooded at high water and during storm surges. The breaking of the waves on the beach on the offshore side of Skallingen generates a south-directed longshore current. The incoming waves propagate partly over the shallow water area to the north and south of the channel and partly through the main

channel itself. In the channel, wave refraction over the shallow water areas is observed, which reduces the wave height significantly. In the shallow water areas, wave energy is reduced by wave breaking and bottom friction effects. The effect of the tidal currents is most apparent in the main channel: the model demonstrates that for an opposing current, the wave height increases and that for a following current it decreases.

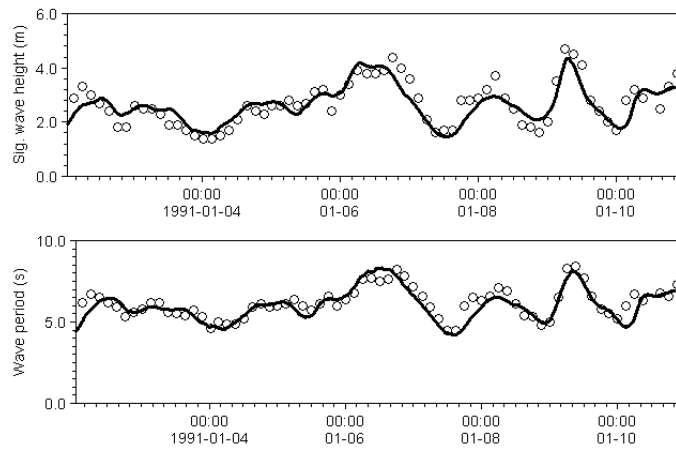


Figure 10. Significant wave height and zero-crossing wave period at St. 2 for the Grådyb tidal inlet case. ● Measurements, — Calculations (instationary formulation).

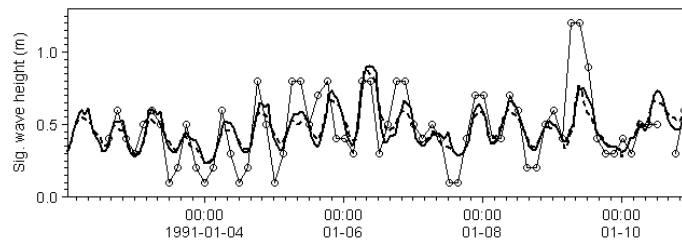


Figure 11. Significant wave height at St. 3 for the Grådyb tidal inlet case. —○— Measurements, — Calculations (instationary formulation) and - - - Calculations (quasi-stationary formulation).

Time series of calculated and measured significant wave height, H_{m0} , and zero-crossing wave period, T_{02} , are compared in Figure 10 for St. 2. It can be seen that there is no significant effect on the wave height from varying water level and current at this location. Figure 11 shows time series of calculated significant wave height, H_{m0} , at St. 3a compared to measurements. Figure 12 shows the calculated

surface elevation and current speed at a location in the center of the channel. At St. 3a there is a significant oscillation of the wave height and the calculated results are in good agreement with the measurements.

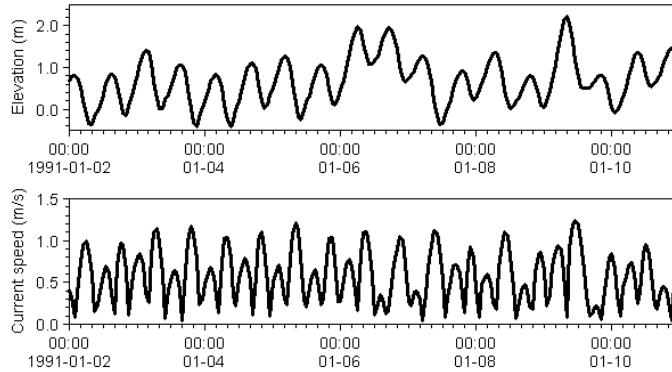


Figure 12. Calculated surface elevation and current speed in the channel in front of St. 3a.

Wave conditions at St. 3a are also influenced by the local generation of wind waves and, therefore, the calculated results are dependent on the air-sea interaction formulation. The use of a coupled formulation (see Komen et al., 1994) for the air-sea interaction gives an overestimation of the wave height. Hence, the results presented here are generated using a decoupled formulation based on a drag law (Smith and Banke 1975). It can be seen (Figures. 11 and 12) that the local maximum of the wave height occurs at maximum opposing current and that the local minimum occurs at maximum following current. The calculated results are very sensitive to the variation in the bathymetry. Hence, the main reason for the deviation between the measured and calculated values is expected to be inaccuracy of the bathymetry.

The coupled simulation was then repeated using the quasi-stationary formulation in the spectral wave model. A time series of significant wave height for St. 3 obtained using this formulation is also included in Figure 12. It can be seen that, even in this case, the difference between instationary and stationary solutions is small.

The average time step used in the instationary wave calculation was 29.6s. The averaged number of iterations required to obtain each quasi-stationary solution was 28. The total CPU time for the instationary and stationary spectral wave calculations was 68.9 and 10.7 hours respectively. In this case study, therefore, an even greater reduction in the CPU time can be achieved using the quasi-stationary solver, without affecting the accuracy of the solution.

CONCLUSION

An integrated numerical modeling system has been presented for applications in areas with large tidal and surge variations and very complex bathymetries. The modeling system contains a dynamic coupling between a 2D flow model and a spectral wave model. The modeling system has been tested in two test areas: The Bristol Channel and the Grådyb tidal inlet. For both cases the calculated results show good agreement with measured data.

The use of a quasi-stationary formulation for the spectral wave model is shown to be a good alternative to the use of an instationary formulation as the computational costs can be reduced significantly.

Simulations using the decoupled parametric formulation in the wave calculations have also been performed as part of this work although not reported in the present paper. These simulations showed that for the Bristol Channel case the prediction of the wave height can be well modeled using the simplified and less computationally demanding approach, but due to the combination of swell and local wind sea the fully spectral approach is needed to accurately predict the wave periods.

REFERENCES

- Andersen, O.B. 1995. Global ocean tides from ERS-1 and TOPEX/POSEIDON altimetry, *J. Geophys Res.* 100 (C12), 25,249-25,259.
- Battjes, J.A. 1972. Radiation stresses in short-crested waves, *J. Mar. Res.* 30, 56-64.
- Battjes, J.A. and J.P.F.M. Janssen, 1978. Energy loss and set-up due to breaking of random waves, *Proc. 16th Int. Conf. Coastal Eng.*, ASCE, 569-587.
- Cefas, 2002. WAVENET directional wave data from 'Lundy wave-rider buoy'.
- Hirsch, C. 1990. *Numerical Computation of Internal and External Flows*, volume 2: Computational Methods for Inviscid and Viscous Flows, Wiley.
- Jawahar P. and H. Kamath. 2000. A high-resolution procedure for Euler and Navier-Stokes computations on unstructured grids, *Journal Comp. Physics*, 164, 165-203.
- Komen, G.J., L. Cavaleri, M. Donelan, K. Hasselmann, S. Hasselmann and P.A.E.M. Janssen. 1994. *Dynamics and Modelling of Ocean Waves*, Cambridge University Press.
- Roe, P. 1981. Approximate Riemann solver, parameter vectors, and difference schemes, *Journal of Computational Physics*, No. 38, 339-374.
- Smith, S.D. and E.G. Banke. 1975. Variation of the sea surface drag coefficient with wind speed. *Quart. J. Roy. Meteor. Soc.*, 101, 665-673.
- Sørensen, O.R., H. Kofoed-Hansen, M. Rugbjerg, and L.S. Sørensen. 2004. A third-generation spectral wave model using an unstructured finite volume technique, *Proceedings of the 29th International Conference on Coastal Engineering 2004*, Lisbon, Portugal.
- Titan Surveys, 2002. GARDLINE data from the Scarweather Sands Wave Tide and Current Monitoring – Sites 1 and 2. Deployment 3.
- U.K. Meteorological Office, 2004. National Centre for Ocean Forecasting. Data from the 'Scarweather wave-rider buoy' 01/06/00 – 31/12/04